Cement & Concrete Composites 31 (2009) 29–38

Contents lists available at ScienceDirect

Cement & Concrete Composites

journal homepage: www.elsevier.com/locate/cemconcomp

Corrosion resistance of self-consolidating concrete in full-scale reinforced beams

A.A.A. Hassan, K.M.A. Hossain, M. Lachemi *

Department of Civil Engineering, Ryerson University, 350 Victoria St, Toronto, ON, Canada M5B 2K3

ARTICLE INFO

Article history:
Received 5 January 2008
Received in revised form 23 October 2008
Accepted 23 October 2008
Available online 13 November 2008

Keywords:
Corrosion
Self-consolidating concrete
Chloride
Durability

ABSTRACT

The corrosion of steel reinforcement embedded in full-scale self-consolidating concrete (SCC) beams was investigated compared to normal concrete (NC). 400 mm width × 363 mm depth × 2340 mm length beams containing epoxy- and non-epoxy-coated stirrups were monitored under an accelerated corrosion test. The corrosion performance of NC/SCC beams was evaluated based on the results of current measurement, half-cell potential tests, chloride ion content, mass loss and bar diameter degradation. The investigation also included the effect of admixture type and the size of specimen on corrosion performance.

In general, SCC beams showed superior performance compared to their NC counterparts in terms of corrosion cracking, corrosion development rate, half-cell potential values, rebar mass loss and rebar diameter reduction. However, SCC beams showed localized corrosion with concrete spalling due to non-uniform concrete properties along the length, which was a result of the casting technique. The results also showed that the difference between SCC and NC mixes in terms of corrosion was more pronounced in large-scale beams, and that types of admixture used in SCC have no influence on corrosion performance.

1. Introduction

The problem of casting concrete in heavily reinforced sections has been a major topic of interest in construction. Proper consolidation and placement of concrete in such heavy reinforced sections require adequate compaction by internal or external mechanical vibrators operated by skilled workers. However, when passing through narrow areas, excessive vibration can lead to segregation, bleeding and blockage of concrete particles. The use of self-consolidating concrete (SCC) is one way to reduce the intensive labor demand for vibration and to alleviate the problems arising from bleeding and segregation. SCC is a highly flowable concrete; it is usually poured from one side of the formwork and spreads under its own weight, filling all spaces and corners until it reaches the other side and levels itself without segregation, and without the use of vibrators for consolidation.

A number of researchers have investigated the uniformity of in situ SCC mixtures in relatively small and large specimens and compared the results with that of normal concrete (NC) mixtures [1–4]. Their studies involved testing cores, pull-out of pre-embedded inserts and/or rebound hammer to evaluate the in situ strength of beams or columns in different locations. Although their conclusion indicated that the in situ SCC mixtures were considerably uniform, their results were based on testing of mechanical properties only; information on testing the variation of durability properties along the length of the element was missing.

Corrosion of steel reinforcement in concrete is a major aspect affecting concrete durability. When concrete is subjected to a chloride-rich environment, the chloride ions can penetrate and diffuse through the body of the concrete, ultimately reaching the steel bars and causing corrosion. Concrete that has low permeability and dense microstructure is believed to obstruct chloride diffusion through the concrete body, which helps reduce the rate of corrosion of embedded reinforcing steel.

SCC is expected to have a dense and less permeable microstructure because of its superior resistance to bleeding and segregation. In addition, segregation and bleeding accompanying excessive vibration are not a factor in SCC. The production of SCC usually involves the use of high range water reducer (HRWR), superplasticizer and/or supplementary cementing materials (SCM). SCM has been proven to increase the concrete corrosion resistance [5–7], while HRWR helps to disperse cement particles in the mix and reduce overall concrete permeability [8,9].

The durability of SCC has been investigated by a number of researchers [10–13] and proved to be excellent. Their investigations involved rapid chloride permeability, water permeation, sulfate resistance/expansion, freezing and thawing and/or deicing salt scaling resistance tests. However, their investigation did not address the durability of SCC in terms of corrosion performance and cracking. Moreover, the investigated SCC samples/specimens in their studies were always relatively small and the durability properties of those samples may not reflect the in situ durability

* Corresponding author. Tel.: +1 416 979 5000; fax: +1 416 979 5122.
E-mail address: mlachemi@ryerson.ca (M. Lachemi).

0958-9465/$ - see front matter © 2008 Elsevier Ltd. All rights reserved.
doi:10.1016/j.cemconcomp.2008.10.005

and uniformity performance of large SCC structural elements such as beams. In general, the effect of segregation and bleeding (which influences durability performance) is more pronounced in large-scale beams when compared to small concrete samples [14]. In addition, the rebar position and casting condition/technique are different than those in the small concrete samples. In large-scale beams, the quality of concrete below lower horizontal bars is expected to be weak and porous due to insufficient compaction and restraint from the horizontal bars in this area [15]. This is likely to occur in full-scale beams rather than in small laboratory samples and would definitely affect concrete durability and rebar corrosion. Therefore, testing the durability of SCC/NC in full-scale beams is essential, since SCC mixes are likely to present distinct advantages over NC in such situations.

The objective of this paper is to investigate the durability performance of full-scale SCC/NC beams in terms of corrosion resistance. This paper also compares the corrosion performance in full-scale beams with that observed in small laboratory cast cylinders to manifest the effect of bleeding, segregation and rebar casting position (that occur in full-size beams rather than small cylinders) on corrosion performance. The corrosion test was carried out using an accelerated corrosion test, in which the concrete samples were partially immersed in sodium chloride solution, and the corrosion rate was monitored by the amount of current passing with time.

2. Research program

The research program described herein was divided into two main stages:

- First stage: studying the corrosion performance in full-scale beams.
- Second stage: studying the corrosion performance in small cylinder specimens.

2.1. First stage: studying the corrosion performance in full-scale beams

This stage was designed to study the corrosion of reinforcement (longitudinal steel and stirrups) and corrosion-induced cracking in full-scale SCC beams compared to representative NC beams. The variation of corrosion performance along the beam length/perimeter was examined to assess the durability of SCC beams. Since corrosion performance is greatly affected by type of admixture, both SCC and NC mixes were made from the same types of admixture and materials. The only differences between the two mixes were the mix design and the addition of high range water reducer in the SCC in order to obtain the required workability.

The beams were divided into two sets: the first set contained non-epoxy-coated stirrup beams investigated until they reached a moderate corrosion level. The second set contained epoxy-coated stirrup beams investigated until they reached a severe corrosion level. The epoxy-coated stirrups were chosen to help study the degradation of beam strength due to longitudinal bar corrosion; that study is not included in this paper. The test for the moderate corrosion level was terminated after either of the two beams (SCC or NC) reached 10% theoretical mass loss of rebar/stirrup. For the severe corrosion level, the test was terminated when either of the two beams reached 30% theoretical rebar/stirrup mass loss.

The corrosion investigation was conducted under accelerated corrosion testing and the corrosion rates were monitored by measuring the current passing with time. The corrosion characteristics along the beam length/perimeter was studied at different locations by taking periodical half-cell potential measurements during the test, as well as chloride ion content near the bar surface, crack patterns and widths, mass loss of rebar/stirrup and reduction of the longitudinal bar diameter at the end of the test.

2.2. Second stage: studying the corrosion performance in small cylinder specimens

This stage focused on the corrosion of reinforcement in small cylinder specimens made with the same NC/SCC mixes used for the first stage. In addition, two other SCC mixtures – similar to the SCC used in the first stage but with different types of high range water reducers – were also used. Accelerated corrosion testing monitored corrosion initiation, corrosion rate, crack patterns and widths during the study period. The primary objective of this stage was to verify the influence of bleeding, segregation and casting technique (which is manifested in full-scale beams rather than small laboratory cylinders) in enhancing SCC durability and corrosion protection. The secondary objective was to investigate the effect of different types of high range water reducers in SCC corrosion protection (if any).

3. Experimental procedure

3.1. Specimen preparation

For the first stage, a total of four concrete beams were used; two made with SCC and two with NC. The four beams were divided into two sets:

- The first set contained one SCC beam and its NC counterpart. Both beams had non-epoxy-coated stirrups in certain locations (three on both sides and one in the middle) and were designed for moderate corrosion levels.
- The second set contained another SCC beam and its NC counterpart with epoxy-coated stirrups (same number and locations as the first set) and were designed for severe corrosion levels.

All beams were 400 mm wide, 363 mm deep and 2340 mm long. The four beams contained three 25 M longitudinal bars at the bottom and two 15 M bars at the top. The longitudinal bar cover was 40 mm, while the cover below stirrups was 30 mm. The beam designation included a combination of letters: SCC or NC to indicate the concrete type, and E or N to indicate the epoxy- and non-epoxy-coated stirrups. For example, a SCC containing epoxy-coated stirrups is designated as SCC-E.

For the second stage, a total of eight concrete cylinders (100 mm in diameter and 200 mm in height), reinforced axially with a single 25 M bar at the centre, were used. The cylinders were divided into four groups of four concrete types. Each group contained two cylinders from each concrete type. The four types were NC and SCC mixes used in the first stage and two other SCC mixes made with two different high range water reducers.

3.2. Materials

Four mixes (one NC and three SCCs) were designed to achieve similar compressive strength. NC and SCC mixes were similar in terms of materials used but had different mix proportions. The main difference between NC and SCC mixes was the coarse aggregate content; SCC had a lower coarse aggregate content (900 kg/m^3) compared to NC (1130 kg/m^3). In addition, SCC mixes had different high range water reducers while NC had none. Details of SCC and NC mix proportions are presented in Table 1.

Type GU Canadian cement similar to ASTM Type I and slag cement were used as cementitious materials for both SCC and NC

Table 1
Mixture proportions for SCC and NC mixtures.

Concrete type	Type GU cement (kg/m^3)	Slag cement (kg/m^3)	10-mm coarse aggregate (kg/m^3)	Fine aggregate (kg/m^3)	Water (kg/m^3)	HRWR mL/100 kg of binder	WR mL/100 kg of binder
SCC	315	135	900	930	180	Variable to obtain similar slump flow	0
NC	300	100	1130	725	160	0	300

mixtures. The chemical and physical properties of cement and slag are presented in Tables 2 and 3, respectively.

Natural sand and 10 mm maximum size stone were used as a fine and coarse aggregates, respectively. High range water reducers similar to Type F of ASTM C 494 [16] and a water reducer (WR) similar to Type A of ASTM C 494 [16] were used to adjust the flowability and cohesiveness of SCC and NC mixtures, respectively. Table 4 presents the fresh properties and the strength of NC and SCC mixtures.

The traditional slump test, according to ASTM C 143/C 143/M [17], was conducted for the NC mixture. The slump flow test [18] was conducted to evaluate the viscosity and flowability of SCC mixture while the V-funnel [19] and L-box [20] tests were conducted to evaluate the stability and the passing ability of SCC, respectively. 100 × 200 mm control cylinders were used to determine the compressive strength (f'_c) and the indirect tensile strength (f'_{ct}) as per ASTM standards C 39/C 39 M and C 39/C 39 M [21,22] for both NC and SCC mixtures. The diameter of deformed bars used for cylinders and the bottom reinforcement of the beams was 25 mm with an average yield strength of 480 MPa and an average tensile strength of 725 MPa.

Table 2
Chemical and physical properties of cement.

Chemical analysis (%)		Physical analysis	
SiO_2	19.64	Residue45 μm (%)	8.42
Al_2O_3	5.48	Blaine fineness (m^2/kg)	410
Fe_2O_3	2.38	Air content (%)	7.78
CaO	62.44	Initial set (min)	103
MgO	2.48	Auto. expansion (%)	0.14
SO_3	4.32	Sulf. expansion (%) (prev. month)	0.013
Total alkali	0.97	–	–
Free lime	1.03	Compressive strength (MPa)	–
LOI	2.05	1 day	19.23
C_3S	52.34	3 days	29.12
C_2S	16.83	7 days	33.82
C_3A	10.50	28 days	41.45
C_4AF	7.24	–	–

Table 3
Chemical and physical properties of slag cement.

Chemical analysis (%)		Physical analysis	
SiO_2	40.3	Residue 45 μm (%)	3.14
Al_2O_3	8.4	Blaine fineness (m^2/kg)	422
Fe_2O_3	0.5	–	–
CaO	38.71	Compressive strength (MPa)	–
MgO	11.06	(50:50 cement:slag)	–
SO_3	0.57	7 days	23.75
K_2O	0.37	28 days	41.96
Na_2O	–	–	–
LOI	0.65	Slag activity index (% of 28 days control)	99.9

3.3. Casting of beam/cylinder specimens

The two concrete mixtures (SCC and NC) used in the first stage were delivered to Ryerson University Structures Laboratory in six-cubic-meter trucks by Dufferin Concrete Group, Toronto, Canada. The delivered SCC mixture was very similar to that successfully used in the Pearson International Airport project in Toronto in 2000 [23].

Immediately after concrete delivery, concrete fresh properties tests were carried out and beams were cast in prepared wooden forms. SCC beams were cast without consolidation; the concrete was poured in the formwork from one end until it flowed and reached the other end. Visual observation showed that the SCC properly filled the forms with ease of movement around reinforcing bars. On the other hand, NC beams were consolidated using electrical vibrators, and trowel-finished for smooth top surfaces. The placement of NC beams was labor-intensive and the time required to cast and finish each beam element was much longer than that required for SCC beams. Formworks were removed after 24 h of casting and the beams were moist-cured for 4 days, then air cured until the date of testing.

The four concrete mixtures used in the second stage were cast in the laboratory using a rotating planetary mixer. The concrete materials were delivered from the same companies as in the first stage to ensure fair comparison between the two stages. The NC mixture was compacted using a vibrating table, while the SCC mixtures did not have any compaction. The concrete cylinders were cured in a similar manner as those in the first stage.

3.4. Accelerated corrosion setup and current measurements

Accelerated corrosion tests have been used successfully to determine the susceptibility of reinforcing and other forms of structural steel to corrosion [24]. The accelerated corrosion setup used in this investigation consisted of plastic tanks, electrolytic solution (5% sodium chloride (NaC1) by the weight of water) and steel mesh placed at the bottom of each tank. Two tanks (2800 mm in length, 1500 mm in width and 500 mm in depth) were used to test the four concrete beams, while the small concrete cylinders were placed in a smaller (700 mm length, 700 mm width and 500 mm depth) tank. Each beam was partially immersed in the electrolytic solution up to one-third of its height (to avoid the corrosion of the top longitudinal bars). The small cylinders were immersed up to two-thirds of their total height. To eliminate any variance in the concentration of the NaC1 and pH

Table 4
Fresh and hardened properties of SCC and NC mixtures.

Concrete type	Slump (mm)	Slump flow		V-funnel flow time (s)	L-box			28-d f'_c (MPa)	28-d f'_{ct} (MPa)
		Flow (mm)	T500 (s)		Index (%)	T200 (s)	T400 (s)		
SCC	–	700	30	5.5	90	1.5	2	45	3.8
NC	80	–	–	–	–	–	–	47	4

T500: flow time to achieve 500-mm slump flow; T200 and T400: times taken by concrete to travel a horizontal distance of 200 mm and 400 mm, respectively.

of the solution, the electrolyte solution was changed on a weekly basis.

The specimen's steel bars and the bottom steel mesh in each tank were connected to a 12 V DC power supply. The direction of the current was arranged so that the steel mesh served as a cathode while the specimen bars served as anodes (Fig. 1). The accelerated corrosion test continued until two degrees of corrosion occured. After the power supply was turned on, the current flowing through the system was recorded at one-hour intervals using a computer-controlled data-acquisition system (Fig. 2). Based on Faraday's Eq. (1), the amount of corrosion is related to the electrical energy consumed and is a function of ampere and time. Therefore, the amount of corrosion can be estimated by using Eq. (1) as follows

$$\text{Mass loss} = \frac{t \times i \times M}{z \times F} \quad (1)$$

where t = the time passed (s), i = the current passed (amperes), M = atomic weight (for iron M = 55.847 g/mol), z = ion charge (two moles of electrons) and F = Faraday's constant which is the amount of electrical charge in one mole of electron (F = 96,487).

Fig. 2. Corrosion current monitoring by data-acquisition system.

3.5. Half-cell potential measurements

This method was first developed in the late 1950s [25] and was adopted in 1977 as an ASTM method C876 [26]. It is based on measuring the electrochemical potential of reinforcement against a reference CSE (copper–copper sulfate electrode) placed on the concrete surface (Fig. 3). The instrument outputs a range of values; more negative values indicate a higher probability of corrosion while positive ones indicate a very low probability of corrosion.

Half-cell potential measurements were taken periodically at 25 different points/locations along the beam length/perimeter. Fig. 4 shows a typical layout of the tested points on each beam. Half-cell potential measurements are usually affected by a number of factors [27], including the moisture condition of the concrete cover and its contamination by carbonation and/or chlorides. The oxygen access strongly determines the half-cell reading; low oxygen content results from a wet surface show low potentials and give higher negative values. Therefore, bi-weekly readings were taken for all beams at the same time and in the same moist surface conditions in order to ensure fair comparison between all beams.

Fig. 3. Half-cell potential measurements.

3.6. Chloride ion measurements

Chloride ion (Cl^-) determination was conducted using a high impedance electrometer with a calibrated chloride electrode to measure the chloride content of concrete powders in the extraction solution as a percentage of concrete mass. Five standard samples containing chloride ranging from 0.005% to 0.5% Cl^- were used to

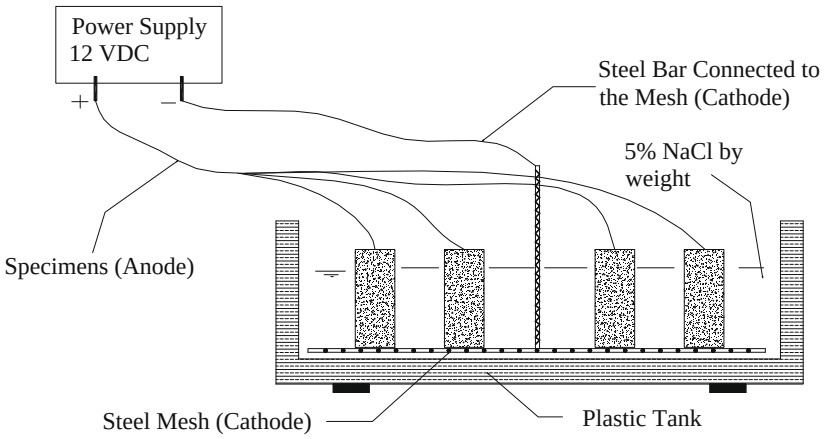

Fig. 1. Schematic representation of the accelerated corrosion test.

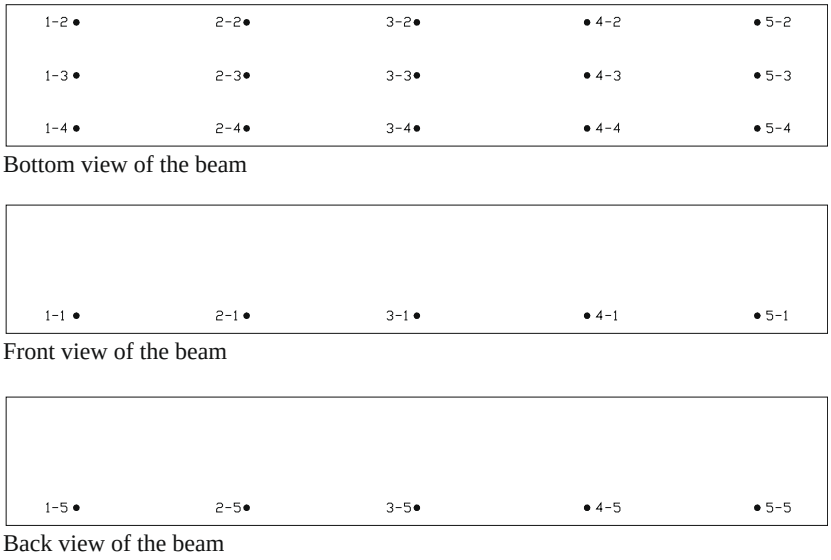

Fig. 4. Typical layout of the tested points along the beam length/perimeter.

calibrate the instrument before use. The concrete powder samples were taken from the same locations near the bar surface using an electrical drill (Fig. 4). The concrete powders were then weighed, poured into small plastic vials containing extraction liquid, and left overnight before testing.

3.7. Measurement of mass loss and reduction of bar diameter

After the beams were corroded and the measurement of half-cell, chloride ion content and crack widths were taken, the beams were jackhammered to remove the corroded stirrups and longitudinal bars. The corroded bars were cleaned with a wire brush to ensure they were free of any adhering concrete or corrosion products, then soaked in a chemical solution (1:1 of HCl and water) according to ASTM Standards G1-03 method [28]. The clean bars were then weighed and the percentage mass loss for each bar was calculated based on Eq. (2):

$$\%\ \text{of mass loss} = \frac{(\text{initial weight} - \text{final weight})}{\text{initial weight}} \times 100 \tag{2}$$

In order to investigate the reduction of bar diameter and mass loss along the length of the beam, each bottom longitudinal bar was cut into five segments to measure mass loss and bar diameter along each segment.

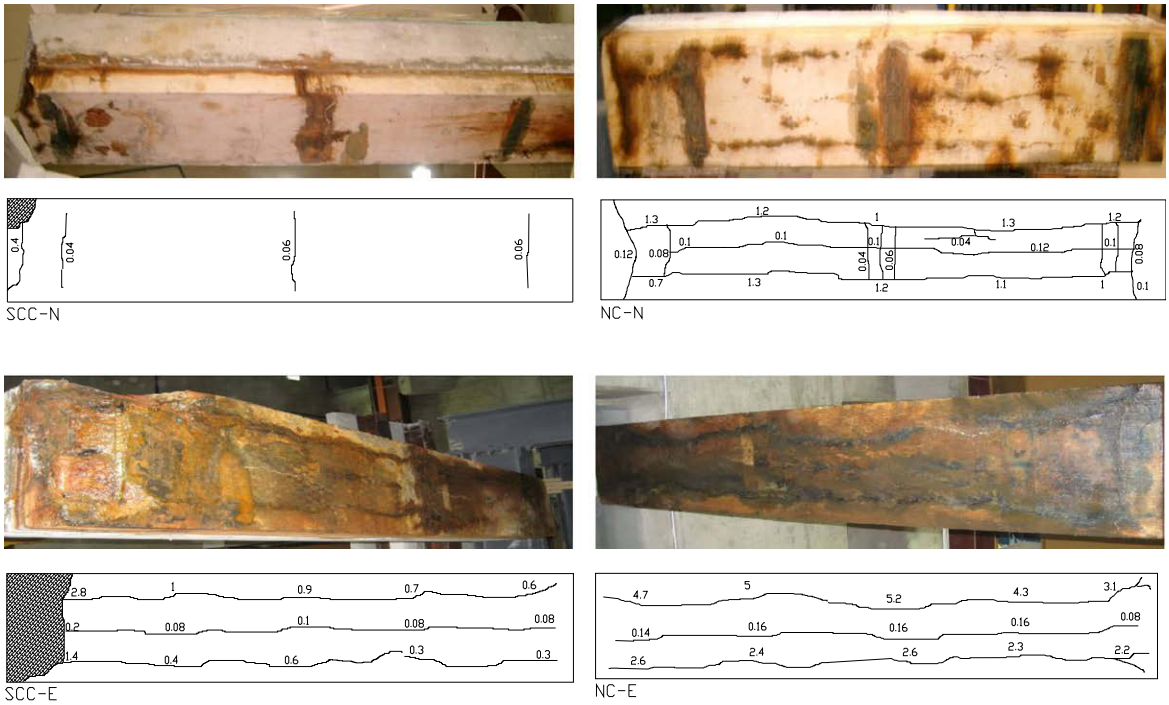

Fig. 5. Corrosion performance, crack pattern and widths (mm) in each tested beam.

4. Experimental results and analysis

4.1. General cracking observation

Fig. 5 shows the crack patterns and crack widths of each tested beam after the completion of corrosion tests. SCC beams exhibited less cracking in terms of number and width than NC beams for both moderate and severe corrosion levels. For example, the SCC-N beam did not have any longitudinal cracking and had minimal transverse cracking at the stirrup location, while the NC-N beam had a number of longitudinal and transverse cracks. Also, the average crack width for the SCC-E beam was around 0.4 mm, while the average crack width for the NC-E beam was around 2.4 mm. This result can be attributed to the higher durability and the superior performance of SCC mixture in rebar corrosion resistance due to its dense and enhanced microstructure.

Fig. 5 also shows that the cracking patterns and widths were not uniformly distributed in SCC beams as they were in NC beams. SCC-N had one broken part at the corner located farthest away from the casting point, while NC-N had uniform cracking patterns and widths along the beam length. Similarly, SCC-E had a big spalled cover at the corner of the beam, which was located far away from the casting point, and the crack width at the bottom of the beam was increasing towards the direction of that corner. Meanwhile, NC-E showed a uniform cracking pattern and had no spalled parts along the beam length. This difference can be attributed to the fact that SCC beams were cast from one end, allowing the concrete to reach the other end under its own weight. The weight of the falling concrete during casting was enough to compact the corner of the beam below the casting point, but not enough to compact it well at the far end. Corners of beams usually require enough compaction due to the restraint of concrete movement from the formworks in three sides. Therefore, SCC beams showed weak and porous concrete at the corners located far away from the casting points.

The results also indicated that SCC beams were easier to break at the aforementioned corners compared to NC beams (which did not break even at corners, with higher crack widths). The reason could be attributed to the fact that the NC mixture contained 25% more coarse aggregate content than the SCC mixture. The higher volume of coarse aggregate in the NC mixture caused higher crack arresting and prevented the concrete from spalling even at corners with higher crack widths.

4.2. Time-dependent corrosion tests results

4.2.1. Current results

During the accelerated corrosion test, the corrosion rate was monitored by a computer-controlled data-acquisition system which recorded the current at 1-h intervals. Figs. 6 and 7 show the relationship between the current in mA and the immersion time in days for SCC/NC beams with epoxy- and non-epoxy-coated stirrups tested for severe and moderate corrosion levels, respectively. In general, the current–immersion time relationship for all beams showed an initial decrease in the current, followed by a gradual increase. The decrease of the current in the first few days is an indication of the formation of the passive film around the reinforcing steel bar, which protects the steel from corrosion. When depassivation of the steel occurs, corrosion starts and then the rate of corrosion increases significantly [29].

NC beams demonstrated higher current values in the early stages of the test, approximately 1.8 and 0.9 mA in NC-N and NC-E, respectively, compared to SCC beams which demonstrated 0.6 and 0.4 mA in SCC-N and SCC-E, respectively. Also, the current in NC beams was higher than that of SCC beams during the whole test

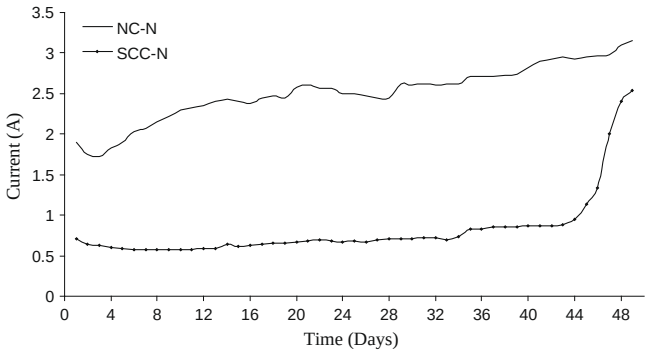

Fig. 6. Current–time history for non-epoxy-coated stirrup beams in moderate corrosion level.

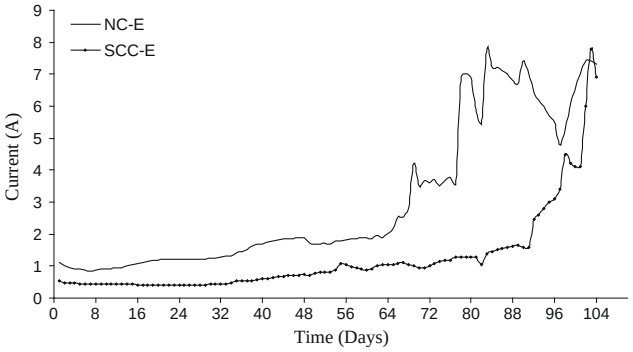

Fig. 7. Current–time history for epoxy-coated stirrup beams in severe corrosion level.

period. The lower current passing through the concrete specimens is an indication of the higher resistivity of the concrete. Permeability of the concrete is the main factor influencing the concrete resistivity [30]. The high flowability and superior resistance to bleeding and segregation of SCC beams were thought to be the main factors that improved the permeability and enhanced the quality of concrete, especially below longitudinal bars.

The point of first increase of the slope in the time–current curve indicates the corrosion initiation, and the slope of the curve represents the rate of corrosion. NC beams showed earlier corrosion initiation and a higher corrosion rate than SCC beams. The corrosion initiation in NC beams started after 3 and 9 days in NC-N and NC-E, respectively, compared to 13 and 30 days in SCC-N and SCC-E beams. The increase of the corrosion initiation time in epoxy-coated compared to non-epoxy-coated stirrup beams was related to the stirrup corrosion, which occurred before longitudinal bar corrosion due to lower cover thickness.

SCC beams exhibited sudden jump in the time–current curve after relatively steady slope compared to NC beams which showed relatively gradual increase of the current with the time. The sudden jump in SCC time–current curves was the indication of the concrete cover spalling in SCC beams at the end corners (Fig. 5).

4.2.2. Half-cell potential measurements

Fig. 8 presents the variation of average cross-section half-cell potential readings along the length of the beams with age. NC showed more negative values compared to SCC in both epoxy- and non-epoxy-coated stirrup beams (moderate and severe corrosion levels). The more negative values in NC beams are an indication of the higher probability of corrosion for NC beams compared

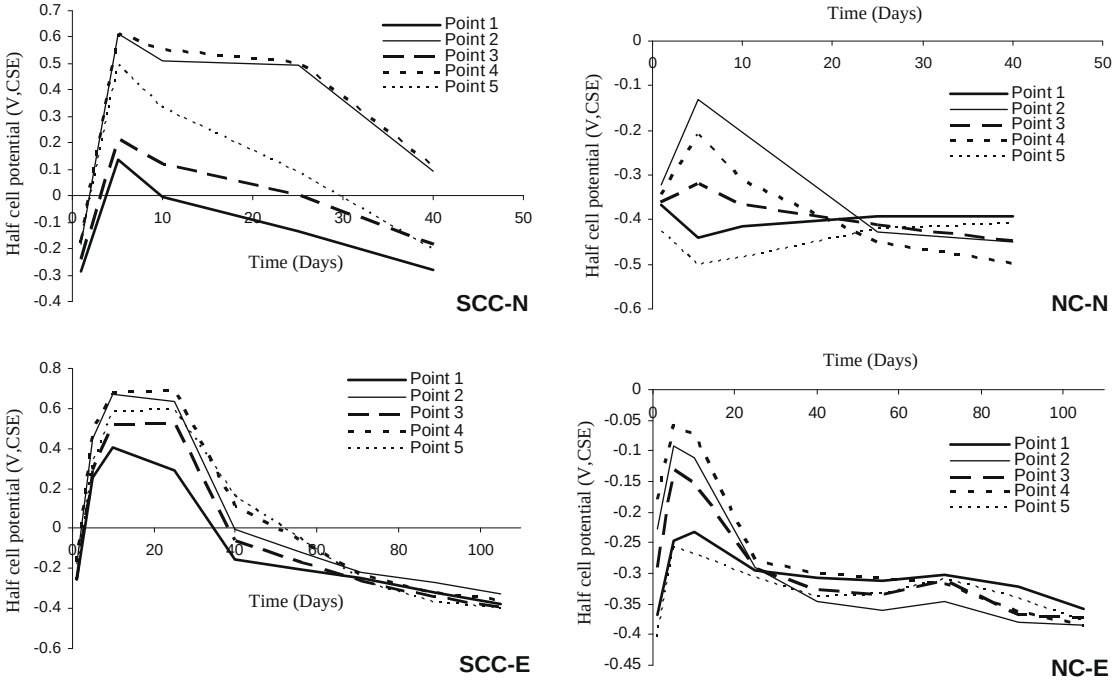

Fig. 8. Average cross-section half-cell reading at each point along the beam length.

to SCC beams. This expectation was verified and confirmed at the end of the test by the other tests' results.

Both SCC and NC beams showed no significant differences in the half-cell readings around the beam cross-sections as it showed along the beam length (Fig. 8). In addition, the readings along the length of the beam for both SCC and NC were dependent on the cover thickness, regardless if the steel underneath was epoxy- or non-epoxy-coated. For example, points 1, 3 and 5 located below stirrups (on any beam, either epoxy- or non-epoxy-coated) that had a 30 mm cover thickness showed more negative values than points 2 and 4, which were not at stirrup location and had a 40 mm cover thickness. This result matched other researchers' results [27] indicating that the concrete cover is a big factor in determining the half-cell potential reading. Also, point 3, located at the middle of any beam, showed less negative value compared to points 1 and 5. This is because point 3 was located below only one stirrup compared to points 1 and 5, which were below three stirrups.

In both epoxy-(E) and non-epoxy-(N) coated stirrup beams, the readings along the length of SCC beams were varied based on the distance from the casting point, while the readings along the length of NC beams did not show any significant differences between the two ends of the beam (Fig. 8). The curves for points 1 and 5 in NC-N and NC-E beams were close to each other, indicating no significant differences between the two ends of the beam. On the other hand, the curves for these two points shifted away in the SCC-N and SCC-E beams, indicating a significant difference between the two beam ends. This result indicates an inferior quality of concrete and a higher probability of corrosion at points far away from casting points in SCC beams.

Fig. 8 also shows that the reading of the half-cell potential test presented closed values at late testing age (high degree of corrosion) compared to early testing age (initial corrosion stage). This result indicates that the half-cell potential test used can only represent the probability of corrosion for uncorroded beams, but may not give good indication for beams that are already corroded.

4.3. Test results after corrosion

4.3.1. Results of chloride content, mass loss and rebar's diameter reduction

Each beam was checked at 25 points/locations along the beam's length/perimeter (Fig. 4). After the completion of the two corrosion levels, the chloride ion content, measurements of crack widths, rebar mass loss and the reduction of the rebar diameter were taken at each location.

Fig. 9 presents the results of the chloride ion content, crack width, mass loss and diameter reduction at each point located on the beam length/perimeter. In general, the chloride ion contents near the longitudinal bar surface at all the points on NC-N and NC-E beams were higher compared to those of SCC-N and SCC-E tested points, respectively. This result confirms the finding of the half-cell and the current monitoring results, which indicated the superior performance of the SCC mixture in protecting the steel bars from corrosion. The chloride ion content was also increased with the increase of the corrosion level (Fig. 9). The corrosion level was indicated by the rebar mass loss or diameter reduction, or by the crack width located close to the tested points. This finding is similar to that found by other researchers [31,32]. It is important to note that, in both NC-N and SCC-N, the chloride ion content was higher at points located below stirrups than at points located below longitudinal bars where the concrete cover is bigger. This result also confirms other researchers' results [32,33] which indicate that the chloride concentration decreases from the concrete surface to the interior in the vicinity of the steel surface.

Fig. 9 revealed the lesser quality of SCC beams at points located far away from the casting point (point 1) compared to better quality of concrete below the casting point (point 5). Chloride ion content, crack width, rebar mass loss and reduction of bar diameter were high at the beam's corner located far away from the casting point, compared to that at the corner located below the casting point (Fig. 9). This result explained the spalling of the concrete cover at the mentioned corners and matched the results of the half-cell potential test during the corrosion-time monitoring.

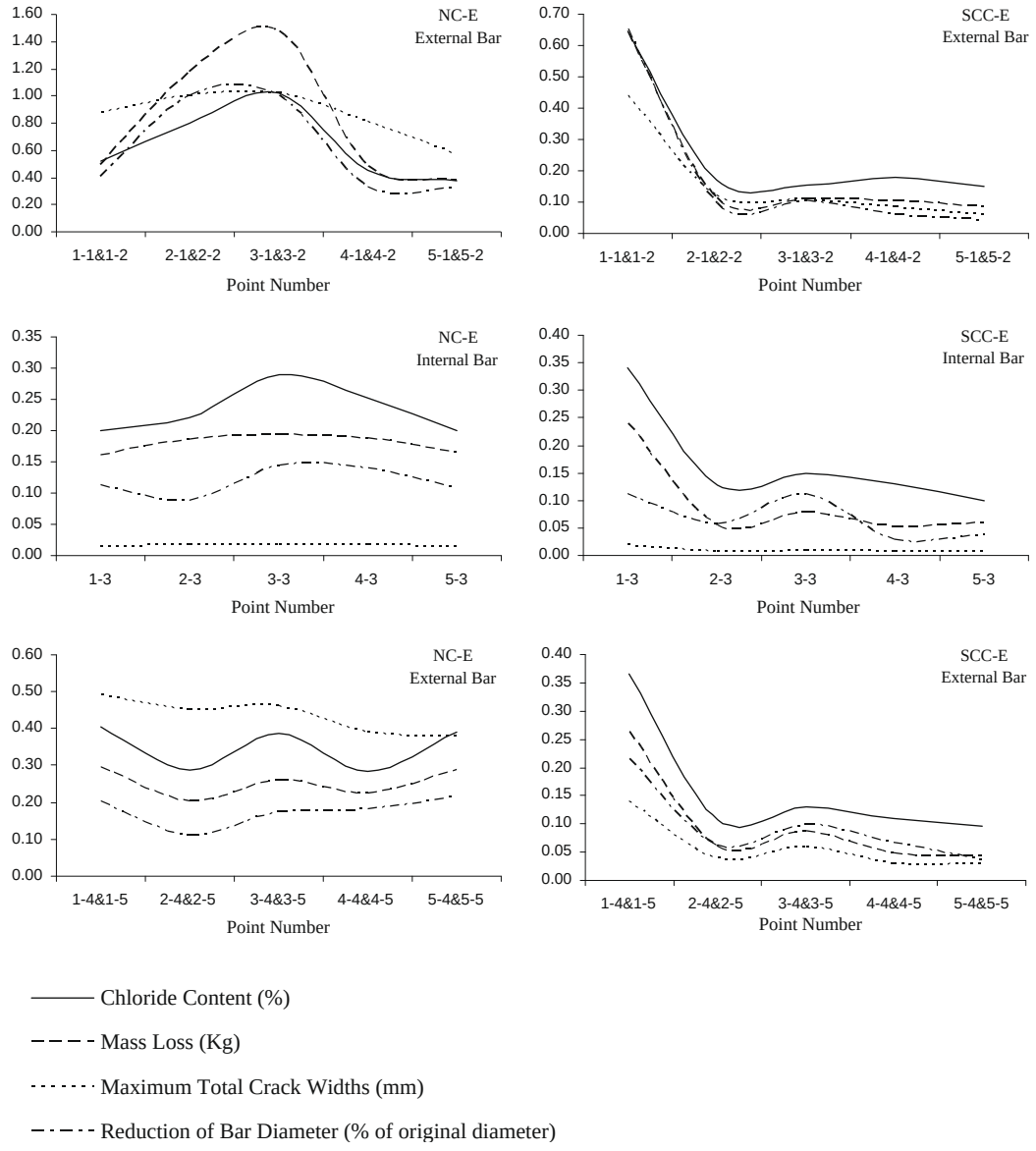

Fig. 9. Chloride content, rebar mass loss, maximum crack width and the reduction of bar diameter along external and internal bars of NC-E and SCC-E.

SCC-N demonstrated no longitudinal cracks, rebar mass loss or diameter reduction at any of its points compared to NC-N, which showed a number of cracks and rebar mass loss and diameter reduction. Also, SCC-E had lower crack widths and less rebar mass loss and diameter reduction in most of its points compared to NC-E. This is another indication of the superior performance of SCC in rebar corrosion protection.

The crack width increased with the increase of the corrosion level in all beam types (Fig. 9). The corrosion products accumulated around the bar surface occupied more space and exerted pressure on the concrete cover, causing cracking. The crack widths increased with the increase of rebar mass loss, except for the middle part of the external bar of NC-E, which showed lower crack width at relatively high mass loss (Fig. 9). This is due to the fact that the entire bar was corroded and diminished at this point.

4.4. Comparison of theoretical and actual corrosion mass loss

The corrosion mass loss was computed using Faraday's Eq. (1) based on the amount electrical energy sent through the bar. The calculated mass loss was compared with the actual mass loss for each of the tested beams after computing the total actual metal loss in the longitudinal bars and stirrups (Fig. 10). The results show

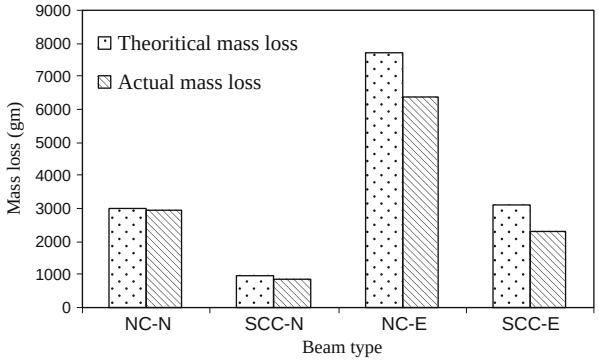

Fig. 10. Comparison of theoretical and actual mass loss in all tested beams.

that the actual mass loss was less than the theoretical mass loss for all tested beams. The percentages of actual to theoretical mass losses were 97%, 91%, 83% and 74% in NC-N, SCC-N, NC-E and SCC-E, respectively. As indicated in previous studies [34,35], when a current passes through a bar suspended in salt solution, the correlation between actual and predicted mass loss is almost perfect, while for bars embedded in concrete, the mass loss based on Faraday's law overestimates the actual mass. This is attributed to the fact that some of the passing currents do not contribute to corrosion but are consumed while passing through the concrete cover.

The results also indicated that the percentage of actual to theoretical mass loss was higher in NC compared to SCC for all tested beams. NC beams corroded faster and developed earlier cracks than SCC beams; these cracks decrease the concrete resistance, resulting in corrosion that is closer to predicted levels [34,35].

4.5. Results of the small concrete cylinder specimens

After evaluating the results of the full-scale beams and confirming the superior performance of SCC compared to NC, it was essential to examine their performance in small concrete cylinders to manifest the effect of bleeding and segregation on durability degradation, and to investigate the effect of different types of HRWR (used in SCC) on the protection of rebar corrosion.

The accelerated corrosion test for the concrete cylinders was terminated after 25 days, when all samples indicated similar corrosion behavior as observed from the crack widths and the current measurement history. Fig. 11 demonstrates one corroded concrete cylinder from each concrete type. As concluded from the current–time measurements, the corrosion initiation time in all concrete types was very close. Also, the rate of corrosion after corrosion initiation was similar in all four concrete mixes. The corrosion initiation time in SCC and NC mixes used in the full-scale concrete beams (first stage) commenced after 13 days of testing, while the other two SCC mixes exhibited corrosion initiation time 2 and 3 days earlier. The crack pattern and crack widths were also similar in the four concrete mixes. All concrete cylinders exhibited one longitudinal crack of a 1 mm width along the length of the embedded bar (Fig. 11).

As expected, bleeding and segregation (associated with large concrete volume and adopted casting/placing/vibrating techniques) were the factors affecting the concrete performance in the full-scale concrete beams where SCC showed superior performance over NC. This was not observed in small cylinder specimens where the bleeding and segregation were minimized and better concrete confinement to embedded bar was ensured compared to the bottom longitudinal bars in the full-scale beams. This is why the small concrete cylinders did not manifest the difference between SCC and NC in rebar corrosion protection. In addition, the close results of the corrosion performance in all SCC mixtures indicate that the HRWR types do not have any chemical effect on corrosion protection.

Fig. 11. Corrosion performance in the small concrete cylinders.

5. Conclusions

The corrosion performance and cracking behavior of self-consolidating concrete (SCC) were described and compared with normal concrete (NC) based on test results of full-scale experimental beams and small-scale concrete cylinders. The current measurements, half-cell potential readings, crack pattern and widths, chloride ion content, rebar mass loss and diameter reduction were critically analyzed to study the influence of SCC mixtures in rebar corrosion protection and durability. Based on the results presented in this paper, the following conclusions were warranted:

- Based on overall performance of the full-scale tested beams, SCC mixture exhibited superior rebar corrosion protection compared to its NC counterpart. Distinct advantages of SCC over NC in terms of corrosion protection were revealed from the results of current measurements with time, crack widths and patterns, half-cell potential measurements, chloride ion contents near the bar surface and the rebar mass loss/diameter reduction.
- The cracks in SCC beams were easily propagated and extended compared to NC beams. SCC beams exhibited breaking and spalling of concrete cover, even at locations which had lower crack widths compared to NC beams. This inferior quality could be attributed to the presence of a lower volume of coarse aggregate in SCC beams (25% less than NC), causing lower crack-arresting capacity that induces concrete spalling even at locations with lower crack widths.
- The SCC mixture showed non-uniform concrete properties along the length of the full-scale concrete beams when casting occurred from one end, causing lesser quality concrete at the far end due to improper compaction and distribution. As a result, severe corrosion and spalling of concrete cover was observed at corners located far away from the casting point. The results of half-cell measurements, crack widths, chloride ion contents, rebar mass loss and rebar diameter reduction confirmed these findings. Therefore, when casting SCC beams, it is recommended that the casting point be moved along the beam length (particularly if the beam is long, shallow and narrow) to ensure uniform compaction, especially at corners.
- Strong correlation between the predicted rebar mass loss by Faraday's equation and experiments suggests that the theoretical estimates can be used to examine the effect of corrosion over time.
- The types of admixture used in SCC mixes have no effect on corrosion performance in terms of corrosion initiation, corrosion rate and crack patterns and widths.

In terms of corrosion performance, the difference between SCC and NC mixes was only pronounced in large-scale concrete beams. No such difference was observed in small-scale cylinder specimens. This difference is due to the fact that the effect of bleeding and segregation (which is less in SCC) was greatly reduced in small-scale cylinders. In addition, the casting technique in small-scale cylinders yields good quality of concrete, especially around the embedded steel bars. This is in comparison to the weaker, more porous layer of concrete (enhanced when using SCC) below the longitudinal bars in the large-scale beams.

Acknowledgements

The authors gratefully acknowledge the financial assistance of the Natural Sciences and Engineering Research Council (NSERC) of Canada and the Canada Research Chair Program. Thanks to Mr. John Pontarollo and Mr. Dennis Baker of St. Lawrence Cement, Canada, for their great support.

References

[1] Khayat KH, Manai K, Trudel A. In situ mechanical properties of wall elements cast using self-consolidating concrete. ACI Mater J 1997;94(6):491–500.
[2] Khayat KH, Tremblay S, Paultre P. Structural response of self-consolidating concrete columns. In: Skarendahl A, Petersson O, editors. Proceedings of the RILEM symposium on self-compacting concrete. Stockholm: RILEM Publications S.A.R.L.; 1999. p. 291–306.
[3] Sonebi M, Tamimi AK, Bartos PJM. Performance and cracking behavior of reinforced beams cast with self-consolidating concrete. ACI Mater J 2003;100(6):492–500.
[4] Zhu W, Gibbs JC, Bartos PJM. Uniformity of in situ properties of self-compacting concrete in full scale structural elements. Cem Concr Compos 2001:57–64.
[5] Hussain S, Rasheeduzzafar. Corrosion resistance performance of fly ash blended cement concrete. ACI Mater J 1994;91(3):264–72.
[6] Al-Amoudi O, Rasheeduzzafar, Maslehuddin M, Al-Mana A. Prediction of long-term corrosion resistance of plain and blended cement concretes. ACI Mater J 1993;90(6):564–70.
[7] Rasheeduzzafar, Al-Saadoun SS, Al-Gahtani AS. Reinforcement corrosion-resisting characteristics of silica-fume blended-cement concrete. ACI Mater J 1992;89(4):337–44.
[8] Haque MN, Kayyali OA. Aspects of chloride ion determination in concrete. ACI Mater J 1995;92(5):532–41.
[9] McCurrich LH. Reduction in permeability and chloride diffusion with superplasticizers. Concrete 1986;20(8):9–10.
[10] Khayat KH. Optimization and performance of air-entrained, self-consolidating concrete. ACI Mater J 2000;97(5):526–35.
[11] Zhu W, Bartos P. Permeation properties of self-compacting concrete. Cem Concr Res 2003:921–6.
[12] Persson B. Internal frost resistance and salt frost scaling of self-compacting concrete. Cem Concr Res 2003;33:373–9.
[13] Nehdi M, Pardhan M, Koshowski S. Durability of self-consolidating concrete incorporating high volume replacement composite cement. Cem Concr Res 2004:2103–12.
[14] Hoshino M. Relationships between bleeding, coarse aggregate, and specimen height of concrete. ACI Mater J 1989;86(2):185–90.
[15] Park R, Paulay T. Reinforced concrete structure. Ultimate strength design of reinforced concrete structures, printed by the University of Canterbury for extension study seminars conducted for practicing structural engineers in New Zealand; 1975:V-1.
[16] ASTM C 494-99a. Standard specification for chemical admixtures for concrete. American Society for Testing and Materials; 2001.
[17] ASTM C 143. Standard test method for slump of hydraulic-cement concrete. American Society for Testing and Materials; 2001.
[18] Nagataki S, Fujiwara H. Self-compacting property of highly flowable concrete. ACI SP 154. Las Vegas (USA): ACI; 1995. p. 301–314.
[19] Ozawa K, Sakata N, Iwai M. Evaluation of self-compactibility of fresh concrete using funnel test. Proc JSCE 1994;490:V-23.
[20] Sonebi M, Batros P, Zhu W, Gibbs J, Tamimi A. Properties of hardened concrete, task 4, final report (2000). Advance Concrete Masonry Center, University of Paisley, Scotland, UK; 2000. p. 6–73.
[21] ASTM C 39. Standard test method for compressive strength of cylindrical concrete specimens. American Society for Testing and Materials; 2001.
[22] ASTM C 496-96. Standard test method for splitting tensile strength of cylindrical concrete specimens. American Society for Testing and Materials; 2001.
[23] Lessard M, Talbot C, Phelan WS, Baker D. Self-consolidating concrete solves challenging placement problems at the Pearson International Airport in Toronto, Canada. In: First North American Conference on the design and use of self-consolidating concrete (SCC), Rosemont, Illinois; 2002. p. 12–13.
[24] Amleh L. Bond deterioration of reinforcing steel in concrete due to corrosion. A thesis submitted to the Faculty of Graduate Studies and Research in partial fulfillment of requirements for the degree of Doctor of Philosophy, McGill University, Montreal, Canada; 2000.
[25] Stratfull RF. The corrosion of steel in a reinforced concrete bridge. Corrosion 1957:173–9.
[26] ASTM C 876. Standard test method for half-cell potentials of uncoated reinforcing steel in concrete. Annual Book of ASTM Standards, American Society for Testing and Materials; 1991.
[27] Klinghoffer O. In situ monitoring of reinforcement corrosion by means of electrochemical methods. Nordic seminar, February 1995.
[28] ASTM G1. Standard practice for preparing, cleaning, and evaluating corrosion test specimens. American Society for Testing and Materials; 2003.
[29] Cornet I, Ishikawa T, Bresler B. The mechanism of steel corrosion in concrete structure. Mater Prot 1968;7(3):44–7.
[30] Hope B, Alan K. Corrosion of steel in concrete made with slag cement. ACI Mater J 1987;84(5):525–31.
[31] Rasheeduzzafar, Ehtesham HS, Al-Saadoun SS. Effect of tricalcium aluminate content of cement on chloride binding and corrosion of reinforcing steel in concrete. ACI Mater J 1992;89(1):3–13.
[32] Amleh L, Mirza S. Corrosion influence on bond between steel and concrete. ACI Struct J 1999;96(3):415–23.
[33] Montemor MF, Cunha MP, Ferreira MG, Simoes AM. Corrosion behavior of rebars in fly ash mortar exposed to carbon dioxide and chlorides. Cem Concr Compos 2002(24):45–53.
[34] Auyeung Y, Balaguru P, Chung L. Bond behavior of corroded reinforcement bars. ACI Mater J 2000;97(2):214–20.
[35] Spainhour LK, Wootton IA. Corrosion process and abatement in reinforced concrete wrapped by fiber reinforced polymer. Cem Concr Compos 2008;30(6):535–43.